JAERI-M
91-110

# OBSERVATION ON EFFECT OF ERGODIC MAGNETIC LIMITER FOR AN OHMIC HEATING PLASMA ON JFT-2M TOKAMAK

July 1991

Hiroshi TAMAI, Teruaki SHOJI, Masahiro MORI, Yukitoshi MIURA
Takaaki FUJITA* and Gerhard FUCHS**

日本原子力研究所
Japan Atomic Energy Research Institute

編集兼発行　日本原子力研究所
印　　　刷　いばらき印刷㈱

JAERI-M 91-110

# Observation on Effect of Ergodic Magnetic Limiter for an Ohmic Heating Plasma on JFT-2M Tokamak

Hiroshi TAMAI, Teruaki SHOJI, Masahiro MORI
Yukitoshi MIURA, Takaaki FUJITA* and Gerhard FUCHS**

Department of Fusion Plasma Research
Naka Fusion Research Establishment
Japan Atomic Energy Research Institute
Naka-machi, Naka-gun, Ibaraki-ken

(Received June 11, 1991)

An ergodic magnetic limiter(EML) is applied to the ohmic heating plasma in JFT-2M tokamak. Different phenomena in plasma behaviour from that during usual ohmic heating phase are reported. Three types of behaviour are observed depending on ergodic field strength and plasma surface q.

The first case corresponds to small EML field, where the maximum attainable density is increased, and the ultimate density linearly increases with the strength of EML field.

In the second case with larger EML field and q value, $H_\alpha$ emission bursts are observed. These bursts coincide with a decrease in density and electron temperature, along with a degradation of plasma confinement.

Thirdly with larger EML field and lower q value, major disruption is triggered. Larger EML field is required for disruption with the increase of the surface q. Larger EML field is also required for the disruption in the discharge of higher plasma current at the constant surface q.

A time delay between the onset of EML coil current and the plasma response is observed, which is consistent with the estimation of the skin

* Research Institute for Applied Mechanics, Kyushu University
** Institut Plasmaphysik EURATOM-KFA, Julich

effect of plasma.

Keywords: Ergodic Magnetic Limiter, JFT-2M Tokamak, Maximum Attainable Density, $H_{\alpha}$-burst, Plasma Major Disruption, Plasma Surface q, Plasma Confinement

# JET－2Mトカマクにおけるオーム加熱時のエルゴディック磁気リミターの効果

日本原子力研究所那珂研究所炉心プラズマ研究部
玉井 広史・荘司 昭朗 ・森 雅博
三浦 幸俊・藤田 隆明* ・Gerhard FUCHS**

（1991年6月11日受理）

エルゴディック磁気リミター（EML）をJET－2Mトカマクのオーム加熱プラズマに印加し，その時のプラズマの振舞いを観測した。

EML を加えたときプラズマは通常のオーム加熱時とは異なる振舞いを示したが，この振舞いは，加えるエルゴディック磁場強度とプラズマ表面のq値により，次の3つの領域に分けられた。

第1の領域はEML磁場強度が比較的小さいときに出現し，最大到達密度が増加した。また，第2，或いは第3の領域に遷移する限界以下のEML 磁場強度においては，EML の強度増加に伴って最大到達密度も増加した。

第2の領域はプラズマ表面のq値とEML 磁場強度が比較的大きい時に出現し，Hα 放射光に大きなバーストが観測された。このバーストは電子密度及び温度の減少に伴って起こり，プラズマ閉じ込め特性の劣化をもたらした。

第3の領域はプラズマ表面のq値が比較的低い時にエルゴディック磁場の増加に伴って出現し，プラズマのディスラプションが引き起こされた。このときプラズマ表面のq値が増加するとディスラプションに要するエルゴディック磁場も増加する。また，表面のq値が一定の下で，プラズマ電流の増加によっても必要なエルゴディック磁場は増加した。

EML コイルの電流を立ち上げてからプラズマにその効果が現れるまで時間遅れが生じたが，この時間遅れはEML の磁場がプラズマ内部に滲み込む際のプラズマの表皮効果を評価した結果と矛盾しない値であった。

---

那珂研究所：〒311－01 茨城県那珂郡那珂町大字向山801－1
＊ 九州大学応用力学研究所
＊＊ EURATOM－KFA，ユーリッヒ研究センター

Contents



目　　次

## 1. Introduction

An ergodic magnetic limiter(EML), which is generated by applying the external resonant magnetic fields, can control the transport and electric field at the edge plasma region[1]-[7]. Effects of EML have been reported for other tokamaks. Increase of thermal transport at the edge plasma region has been observed in TEXT[1]. Ergodization of internal islands has been achieved in TORIUT-4M[2]. The expected magnetic geometry in many poloidal harmonics has been confirmed by electron beam probing in CSTN-II[3]. In TEXTOR[4], formation of stationary magnetic islands at the plasma edge has enhanced the $H_\alpha$ and impurity emission.

In JFT-2M tokamak, EML experiments have been aiming for an increase of density limit, and for achieving a steady state H-mode[5][6][7].

In this report, the response of the ohmic heating plasma by EML is discussed. Three different phenomena are observed depending on the strength of EML field and on the q value. Regions and experimental conditions for those phenomena are discussed. The experimental arrangement of EML field is described in Section 2, each phenomenon is presented in Section 3, finally, experimental results are summarized in Section 4.

## 2. Experimental Setup of EML Field

The location of EML coils on the torus is shown in Fig.1. The coils are located outside the vacuum vessel. Three sets of three coils are located at toroidal angle of 0°, 158°, and 180°. At each toroidal position, the coils are located poloidally at -40°, 0°, and 40° to the midplane.

The mode number of EML is determined by the current direction in each coil. A high-*m* mode is formed when all coils of a poloidal section have the same current direction, and a low-*m* mode is formed when current in the central coil flows in reverse direction. Toroidal mode number, *n*, can be changed from even to odd by changing the current direction in the coils at different toroidal locations. The poloidal mode spectrum is obtained by the Fourier analysis. The spectrum is relatively broad and has a peak at $m$=5 and $m$=11 near the plasma edge for low-*m* and high-*m* mode, respectively[5].

Width of magnetic island generated by EML current is calculated by a field line tracing code which assumes a q-profile[7][8]. Figure 2 is an example of the calculation for the current dependence of island width in the case of surface q of 4.5. Islands within normalized flux between 0.6 and 1.0 are shown. Small numbers at the left side of figures indicate the set of poloidal/toroidal mode number $m/n$. Island width increases with increasing EML current, and in

## 1. Introduction

An ergodic magnetic limiter(EML), which is generated by applying the external resonant magnetic fields, can control the transport and electric field at the edge plasma region[1]-[7]. Effects of EML have been reported for other tokamaks. Increase of thermal transport at the edge plasma region has been observed in TEXT[1]. Ergodization of internal islands has been achieved in TORIUT-4M[2]. The expected magnetic geometry in many poloidal harmonics has been confirmed by electron beam probing in CSTN-II[3]. In TEXTOR[4], formation of stationary magnetic islands at the plasma edge has enhanced the $H_\alpha$ and impurity emission.

In JFT-2M tokamak, EML experiments have been aiming for an increase of density limit, and for achieving a steady state H-mode[5][6][7].

In this report, the response of the ohmic heating plasma by EML is discussed. Three different phenomena are observed depending on the strength of EML field and on the q value. Regions and experimental conditions for those phenomena are discussed. The experimental arrangement of EML field is described in Section 2, each phenomenon is presented in Section 3, finally, experimental results are summarized in Section 4.

## 2. Experimental Setup of EML Field

The location of EML coils on the torus is shown in Fig.1. The coils are located outside the vacuum vessel. Three sets of three coils are located at toroidal angle of 0°, 158°, and 180°. At each toroidal position, the coils are located poloidally at -40°, 0°, and 40° to the midplane.

The mode number of EML is determined by the current direction in each coil. A high-*m* mode is formed when all coils of a poloidal section have the same current direction, and a low-*m* mode is formed when current in the central coil flows in reverse direction. Toroidal mode number, $n$, can be changed from even to odd by changing the current direction in the coils at different toroidal locations. The poloidal mode spectrum is obtained by the Fourier analysis. The spectrum is relatively broad and has a peak at $m$=5 and $m$=11 near the plasma edge for low-*m* and high-*m* mode, respectively[5].

Width of magnetic island generated by EML current is calculated by a field line tracing code which assumes a q-profile[7][8]. Figure 2 is an example of the calculation for the current dependence of island width in the case of surface q of 4.5. Islands within normalized flux between 0.6 and 1.0 are shown. Small numbers at the left side of figures indicate the set of poloidal/toroidal mode number $m/n$. Island width increases with increasing EML current, and in low-*m* mode there exist relatively larger islands than those in high-*m* mode. At higher EML current, overlapping of the magnetic islands occurs.

The effects of EML field are observed in the ohmic phase of D-shaped hydrogen plasma with limiter configuration.

## 3. Results and Discussions

### *3.1 Increase of maximum attainable density*

In Fig. 3, the increase of the maximum attainable density by applying EML field is reviewed. An EML of low-*m*/even mode is applied to the ohmic plasma with a current of 230kA and plasma surface q of 5.0. The surface q is determined by the q value at 5mm inside the separatrix using the magnetic fitting calculation[9]. Without EML, the density limit is around $2.9 \times 10^{19} m^{-3}$, and MHD activity, measured by the magnetic probes, is large. With EML the density limit is increased to about $3.6 \times 10^{19} m^{-3}$ and the MHD activity is reduced.

Maximum attainable density, $\bar{n}_e^{max}$, depends on the surface q, $q_s$, as well as on the strength of EML field. Figure 4 shows the dependence of $\bar{n}_e^{max}$ on EML current. The plasma current is 230kA and EML operates with low-*m*/even mode, in which dominant spectrum is $m/n$=7/2. Circles, triangles, and squares show the case of surface q of 3.2, 4.0, and 5.0, respectively. The surface q is varied by changing the toroidal magnetic field. In the case of $q_s$=5.0, the maximum attainable density increases with EML current. On the other hand, no increase in $\bar{n}_e^{max}$ is observed in the case of $q_s$=3.2, which is smaller than the resonance value determined by the dominant component of EML spectrum $m/n$ of 3.5. These results suggest that the resonance of EML field, defined by dominant component, would have to exist inside the plasma in order to improve the maximum attainable density.

### *3.2 Appearance of $H_\alpha$-burst*

With an increase of EML current, frequent large bursts in $H_\alpha$ emission are observed. Figure 5 shows the temporal behaviour of plasma parameters in D-shaped limiter discharge with q value of 4.7 where EML of low-*m*/even mode is used at 0.6s with duration of 0.4s. Soon after the turn-on of EML current, bursts of $H_\alpha$ emission begin and continue during whole phase of EML. In the burst phase, averaged electron density and stored energy($W_s$) decrease, which indicates a degradation of particle and energy confinement by EML. The decrease of energy confinement time is roughly estimated to be from 40ms to 30ms when applying the EML field. Electron temperature($T_e$), observed by electron cyclotron emission(ECE), decreases at r=0.75*a*, but remains unchanged at low-*m* mode there exist relatively larger islands than those in high-*m* mode. At higher EML current, overlapping of the magnetic islands occurs.

The effects of EML field are observed in the ohmic phase of D-shaped hydrogen plasma with limiter configuration.

## 3. Results and Discussions

### *3.1 Increase of maximum attainable density*

In Fig. 3, the increase of the maximum attainable density by applying EML field is reviewed. An EML of low-*m*/even mode is applied to the ohmic plasma with a current of 230kA and plasma surface q of 5.0. The surface q is determined by the q value at 5mm inside the separatrix using the magnetic fitting calculation[9]. Without EML, the density limit is around $2.9 \times 10^{19} m^{-3}$, and MHD activity, measured by the magnetic probes, is large. With EML the density limit is increased to about $3.6 \times 10^{19} m^{-3}$ and the MHD activity is reduced.

Maximum attainable density, $\bar{n}_e^{max}$, depends on the surface q, $q_s$, as well as on the strength of EML field. Figure 4 shows the dependence of $\bar{n}_e^{max}$ on EML current. The plasma current is 230kA and EML operates with low-*m*/even mode, in which dominant spectrum is $m/n$=7/2. Circles, triangles, and squares show the case of surface q of 3.2, 4.0, and 5.0, respectively. The surface q is varied by changing the toroidal magnetic field. In the case of $q_s$=5.0, the maximum attainable density increases with EML current. On the other hand, no increase in $\bar{n}_e^{max}$ is observed in the case of $q_s$=3.2, which is smaller than the resonance value determined by the dominant component of EML spectrum $m/n$ of 3.5. These results suggest that the resonance of EML field, defined by dominant component, would have to exist inside the plasma in order to improve the maximum attainable density.

### *3.2 Appearance of $H_\alpha$-burst*

With an increase of EML current, frequent large bursts in $H_\alpha$ emission are observed. Figure 5 shows the temporal behaviour of plasma parameters in D-shaped limiter discharge with q value of 4.7 where EML of low-*m*/even mode is used at 0.6s with duration of 0.4s. Soon after the turn-on of EML current, bursts of $H_\alpha$ emission begin and continue during whole phase of EML. In the burst phase, averaged electron density and stored energy($W_s$) decrease, which indicates a degradation of particle and energy confinement by EML. The decrease of energy confinement time is roughly estimated to be from 40ms to 30ms when applying the EML field. Electron temperature($T_e$), observed by electron cyclotron emission(ECE), decreases at r=0.75*a*, but remains unchanged at r=0.43$a$; where $a$ is the plasma minor radius.

The profile of electron temperature is shown in Fig.6. Open and solid circles show the temperature averaged over 10ms without EML(t=0.6s), and that with EML(t=0.8s), respectively. By applying EML field, not only the electron temperature at the edge but also that at the centre decreases.

Figure 7 shows the blew-up of temporal behaviour of $H_\alpha$ emission and electron temperature for the shot shown in Fig.5. At the onset of $H_\alpha$-burst, the electron temperature at r=0.75$a$, and 0.88$a$ jumps up; on the other hand, that at r=0.21$a$, 0.43$a$, and 0.59$a$ drops down. The change in electron temperature initially starts at the edge plasma region, and subsequently the electron temperature at the central region follows. Thus, the change in electron temperature during the $H_\alpha$-burst has a different feature from the normal sawtooth activity. The $H_\alpha$-burst is similar to the edge localized mode(ELM), which is obtained during H-mode phase in marginal input power[6], since in the ELM phase the periodic change of the $H_\alpha$ emission is also observed with modification of plasma profile and with the degradation of plasma confinement[10]. However, it has not yet been well investigated whether the present $H_\alpha$-burst would be the same phenomenon as ELM, and why $H_\alpha$-burst occurs in ohmic heating phase. Further observations are required to clarify the operational condition and the mechanism of appearance in present $H_\alpha$-burst phenomenon.

### *3.3 Regions of phenomena in an $I_{EML}$-$q_s$ plane*

Operation at relatively lower surface q and larger EML field results in plasma disruption.

Those phenomena described above are observed in a operational range defined by the strength of EML field and the plasma surface q. Figure 8 shows the regions of improvement of maximum density, appearance of $H_\alpha$-burst, and major plasma disruption, in the plane of EML current($I_{EML}$) versus surface q($q_s$). Plasma current is 230kA and EML operates with low-$m$/even mode. Open and solid circles show the marginal EML coil current for the appearance of $H_\alpha$-burst, and for the plasma disruption, respectively. Hatched area indicates no improvement of maximum attainable density as shown in Fig.4. The surface q is scanned by changing the strength of the toroidal magnetic field.

At a constant surface q, maximum attainable density increases as EML current increases. However, beyond the marginal EML current, frequent large bursts of $H_\alpha$ emission are triggered in the case of higher surface q greater than 4; on the other hand, major disruption is induced in the case of lower surface q smaller than 4. This is suggestive of large magnetic islands, generated inside the plasma, which would induce the disruption or degradation of plasma confinement.

### *3.4 Major plasma disruption*

Since the plasma is relatively stable against disruption in the case of high-*m* mode operation, the strength of EML field and the plasma surface q are surveyed in the high-*m* poloidal mode number in order to investigate the operational regime related to the major plasma disruption.

In Fig.9 EML current with high-*m* mode is plotted against the plasma surface q for cases with disruption, and without disruption. Plasma current is fixed at 230kA, and the strength of the toroidal magnetic field is scanned. Circles and squares represent the toroidal mode of even, and odd number, respectively; open and solid symbols indicate the case without, and with disruption, respectively.

At lower surface q, the required EML coil current for disruption becomes smaller. The disruption still occurs when there is no resonance inside the plasma for the dominant component of the EML spectrum of $m/n$=12/4 in even mode and for that of $m/n$=12/3 in odd mode. This is opposite tendency against that of density maximum improvement. There is a possibility that another small fraction of EML spectrum would have a resonance inside the plasma, and would cause the disruption in the low-q plasma.

Figure 10 shows the minimum EML coil current for the disruption against the plasma current. The EML operates in a high-*m*/odd mode, and surface q is fixed at 3.5. The EML field and given plasma current are roughly proportional. However, more precise estimations and observations would be required to ascertain how the magnetic perturbation depends on the plasma current, and how the plasma interacts with EML field.

### *3.5 Plasma skin effect*

The threshold EML coil current for the appearance of $H_\alpha$-burst appears to depend on the flat top of EML coil current. Fig.11 shows the temporal evolution of EML coil current and the time point(crosses) of the onset in $H_\alpha$-bursts in EML of low-*m*/even mode. In the case of EML flat top current of 5kA, $H_\alpha$-burst appears at the current of nearly 4kA; it appears at about 2.3kA in the case of EML flat top of 3kA. The rise time of coil current in 5kA is shorter than in 3kA case. This suggest that the appearance of $H_\alpha$-burst depends not only on coil current but also on the current rise rate. This may be due to a skin effect of plasma.

The time delay is roughly estimated using the model of skin effect in metal surface; that is given by $d_{max}^2 < 1/\pi\sigma f\mu$, where $d_{max}$, $\sigma$, $f$, $\mu$ are the maximum penetration depth and electrical conductivity of the material, frequency of magnetic field, and the magnetic permeability, respectively.

Conductivity $\sigma$ is estimated to about $4.58\times10^5(\Omega m)^{-1}$ by plasma resistivity at effective $Z$ of 2, electron density and temperature of $1\times10^{19}m^{-3}$, and 0.1keV, respectively. Maximum penetration depth is assumed to be the distance between the plasma surface and the resonance radius for EML. The dominant resonance of EML is assumed to be at $r=0.7a$ where the change of electron temperature, shown in Fig.6, is nearly maximum; A penetration depth of about 10cm is then estimated. Under those assumptions the frequency of $f < 55$Hz is obtained, and rising time of $\tau > 18$ms is deduced. If the real threshold EML coil current for appearance of $H_\alpha$-burst is assumed to be 2.3kA, the time delay is estimated about 27ms in Fig.11; which is consistent with the model estimation in order of magnitude.

Thus, the time delay between the onset of EML coil current and the start of $H_\alpha$-burst could be attributed to a plasma skin effect.

## 4. Conclusions

Confinement properties of the ohmic heating plasma with the ergodic magnetic limiter are investigated in JFT-2M tokamak.

Depending on the strength of the EML field and on the plasma surface q, there exist three regions in an $I_{EML}$-$q_s$ plane in which the plasma behaviour is clearly characterized.

In the first region the maximum attainable density is increased, and the ultimate density linearly increases with the strength of EML field. Effects of EML field only appears when the resonance of dominant EML spectrum component is located inside the plasma.

In the second region, which is associated with larger strength of EML field and relatively higher surface q, large bursts of $H_\alpha$ emission are observed, and degradation of the plasma confinement occurs. A significant drop in the electron temperature is observed during $H_\alpha$-burst phase. This phenomenon is similar to the ELM, but has not been well analyzed yet.

In the third region by larger EML field and relatively lower surface q, major plasma disruptions are induced. Required EML field for the disruption depends on the plasma surface q and on the intensity of plasma current. Disruption still occurs at low-q where there is no resonance for dominant EML a skin effect of plasma.

The time delay is roughly estimated using the model of skin effect in metal surface; that is given by $d_{max}^2 < 1/\pi\sigma f\mu$, where $d_{max}$, $\sigma$, $f$, $\mu$ are the maximum penetration depth and electrical conductivity of the material, frequency of magnetic field, and the magnetic permeability, respectively.

Conductivity $\sigma$ is estimated to about $4.58\text{x}10^5(\Omega\text{m})^{-1}$ by plasma resistivity at effective $Z$ of 2, electron density and temperature of $1\text{x}10^{19}\text{m}^{-3}$, and 0.1keV, respectively. Maximum penetration depth is assumed to be the distance between the plasma surface and the resonance radius for EML. The dominant resonance of EML is assumed to be at $r=0.7a$ where the change of electron temperature, shown in Fig.6, is nearly maximum; A penetration depth of about 10cm is then estimated. Under those assumptions the frequency of $f < 55$Hz is obtained, and rising time of $\tau > 18$ms is deduced. If the real threshold EML coil current for appearance of $H_\alpha$-burst is assumed to be 2.3kA, the time delay is estimated about 27ms in Fig.11; which is consistent with the model estimation in order of magnitude.

Thus, the time delay between the onset of EML coil current and the start of $H_\alpha$-burst could be attributed to a plasma skin effect.

## 4. Conclusions

Confinement properties of the ohmic heating plasma with the ergodic magnetic limiter are investigated in JFT-2M tokamak.

Depending on the strength of the EML field and on the plasma surface q, there exist three regions in an $I_{EML}$-$q_s$ plane in which the plasma behaviour is clearly characterized.

In the first region the maximum attainable density is increased, and the ultimate density linearly increases with the strength of EML field. Effects of EML field only appears when the resonance of dominant EML spectrum component is located inside the plasma.

In the second region, which is associated with larger strength of EML field and relatively higher surface q, large bursts of $H_\alpha$ emission are observed, and degradation of the plasma confinement occurs. A significant drop in the electron temperature is observed during $H_\alpha$-burst phase. This phenomenon is similar to the ELM, but has not been well analyzed yet.

In the third region by larger EML field and relatively lower surface q, major plasma disruptions are induced. Required EML field for the disruption depends on the plasma surface q and on the intensity of plasma current. Disruption still occurs at low-q where there is no resonance for dominant EML

spectrum component inside the plasma; the cause has been not clear.

There exists a time delay for triggering the $H_\alpha$-burst, and the time delay is consistent with the estimation of plasma skin effect.

Acknowledgement

The authors are grateful to the members of the Experimental Plasma Physics Laboratory for their constructive advice and fruitful discussion. They also thank the members of JFT-2M Facility Division for their excellent co-operation and helpful support. They are indebted to Drs. H.Maeda, S.Tamura, T.Iijima, M.Yoshikawa, and M.Tanaka for their continuous encouragement.

References

[1] S.C.Mccool *et al.*, Nucl. Fusion *29* (1989) 547.

[2] K.Hattori, *et al.*, J. Nucl. Mater. *121* (1984) 368.

[3] S.Takamura, *et al.*, Phys. Fluids *30* (1987) 144.

[4] G.Fuchs in *Controlled Fusion and Plasma Heating* (Proc.13th Europ. Conf.Schliersee,1986) Part I, European Physical Society (1986) 427.

[5] T.Shoji *et al.*, in *Controlled Fusion and Plasma Physics* (Proc.17th Europ.Conf.Amsterdam,1990) Part III, European Physical Society (1990) 1452.

[6] Y.Miura *et al.*, in *Plasma Physics and Controlled Nuclear Fusion Research* (13th Int.Conf.Washington,1990 IAEA-CN-53/A-4-6).

[7] A.W.Leonard *et al.*, "The Effects of Applied Error Fields on the H-mode Plasmas of JFT-2M" *to be published in Nucl.Fusion.*

[8] A.H.Boozer Phys. Fluids *27*(1984) 2055.

[9] M.Mori *et al.*, Nucl. Fusion *27* (1987) 725.

[10] H.Matsumoto *et al.*, Nucl. Fusion *31* (1991) 93.

spectrum component inside the plasma; the cause has been not clear.

There exists a time delay for triggering the $H_\alpha$-burst, and the time delay is consistent with the estimation of plasma skin effect.

Acknowledgement

The authors are grateful to the members of the Experimental Plasma Physics Laboratory for their constructive advice and fruitful discussion. They also thank the members of JFT-2M Facility Division for their excellent co-operation and helpful support. They are indebted to Drs. H.Maeda, S.Tamura, T.Iijima, M.Yoshikawa, and M.Tanaka for their continuous encouragement.

References

[1] S.C.Mccool *et al.*, Nucl. Fusion *29* (1989) 547.

[2] K.Hattori, *et al.*, J. Nucl. Mater. *121* (1984) 368.

[3] S.Takamura, *et al.*, Phys. Fluids *30* (1987) 144.

[4] G.Fuchs in *Controlled Fusion and Plasma Heating* (Proc.13th Europ. Conf.Schliersee,1986) Part I, European Physical Society (1986) 427.

[5] T.Shoji *et al.*, in *Controlled Fusion and Plasma Physics* (Proc.17th Europ.Conf.Amsterdam,1990) Part III, European Physical Society (1990) 1452.

[6] Y.Miura *et al.*, in *Plasma Physics and Controlled Nuclear Fusion Research* (13th Int.Conf.Washington,1990 IAEA-CN-53/A-4-6).

[7] A.W.Leonard *et al.*, "The Effects of Applied Error Fields on the H-mode Plasmas of JFT-2M" *to be published in Nucl.Fusion.*

[8] A.H.Boozer Phys. Fluids *27*(1984) 2055.

[9] M.Mori *et al.*, Nucl. Fusion *27* (1987) 725.

[10] H.Matsumoto *et al.*, Nucl. Fusion *31* (1991) 93.

spectrum component inside the plasma; the cause has been not clear.

There exists a time delay for triggering the $H_\alpha$-burst, and the time delay is consistent with the estimation of plasma skin effect.

Acknowledgement

The authors are grateful to the members of the Experimental Plasma Physics Laboratory for their constructive advice and fruitful discussion. They also thank the members of JFT-2M Facility Division for their excellent co-operation and helpful support. They are indebted to Drs. H.Maeda, S.Tamura, T.Iijima, M.Yoshikawa, and M.Tanaka for their continuous encouragement.

References

[1] S.C.Mccool *et al.*, Nucl. Fusion *29* (1989) 547.
[2] K.Hattori, *et al.*, J. Nucl. Mater. *121* (1984) 368.
[3] S.Takamura, *et al.*, Phys. Fluids *30* (1987) 144.
[4] G.Fuchs in *Controlled Fusion and Plasma Heating* (Proc.13th Europ. Conf.Schliersee,1986) Part I, European Physical Society (1986) 427.
[5] T.Shoji *et al.*, in *Controlled Fusion and Plasma Physics* (Proc.17th Europ.Conf.Amsterdam,1990) Part III, European Physical Society (1990) 1452.
[6] Y.Miura *et al.*, in *Plasma Physics and Controlled Nuclear Fusion Research* (13th Int.Conf.Washington,1990 IAEA-CN-53/A-4-6).
[7] A.W.Leonard *et al.*, "The Effects of Applied Error Fields on the H-mode Plasmas of JFT-2M" *to be published in Nucl.Fusion.*
[8] A.H.Boozer Phys. Fluids *27*(1984) 2055.
[9] M.Mori *et al.*, Nucl. Fusion *27* (1987) 725.
[10] H.Matsumoto *et al.*, Nucl. Fusion *31* (1991) 93.

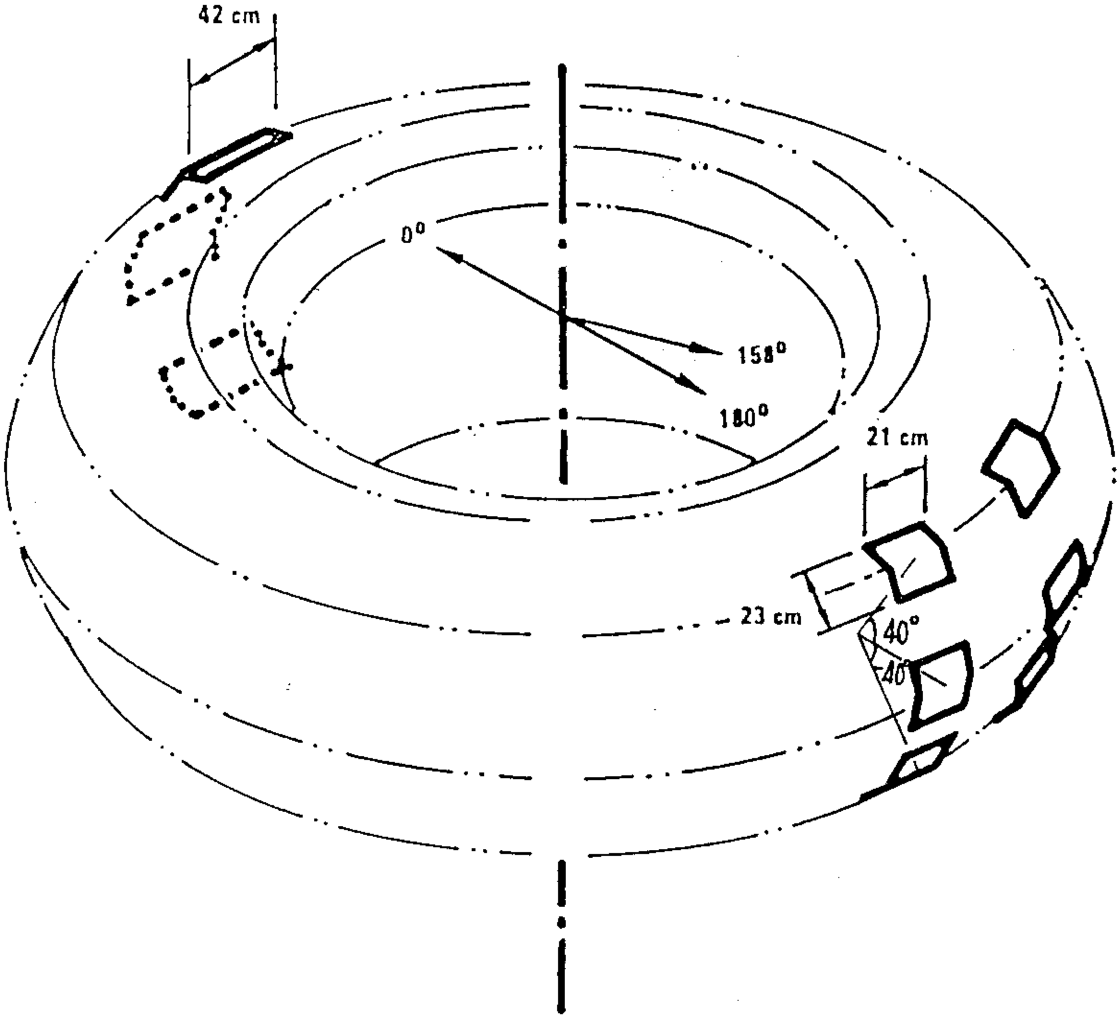


Fig. 1 Location of EML coils on the torus. Three sets of three coils are located at toroidal angle of 0°, 158°, and 180°. At each toroidal position, the coils are located poloidally at -40°, 0°, and 40° to the midplane. (from Reference [7])

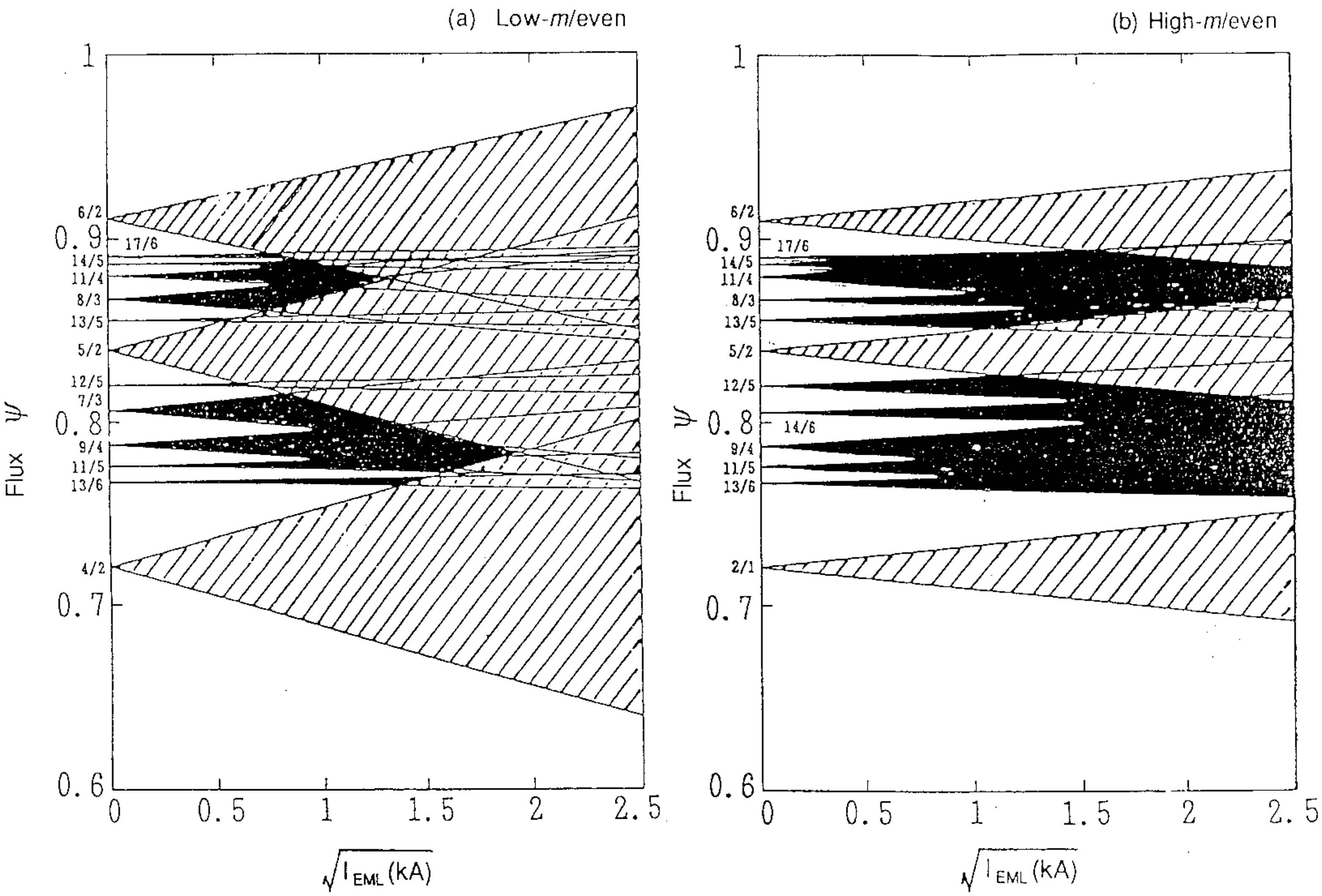


Fig. 2 Dependence of magnetic island width on the EML coil current with poloidal/toroidal mode of (a) low-m/even and of (b) high-m/even. Island width is calculated by a field line tracing code with an assuming q-profile and surface q of 4.5. Small number at the left side indicates the set of poloidal and toroidal mode number m/n. (from Reference [5])

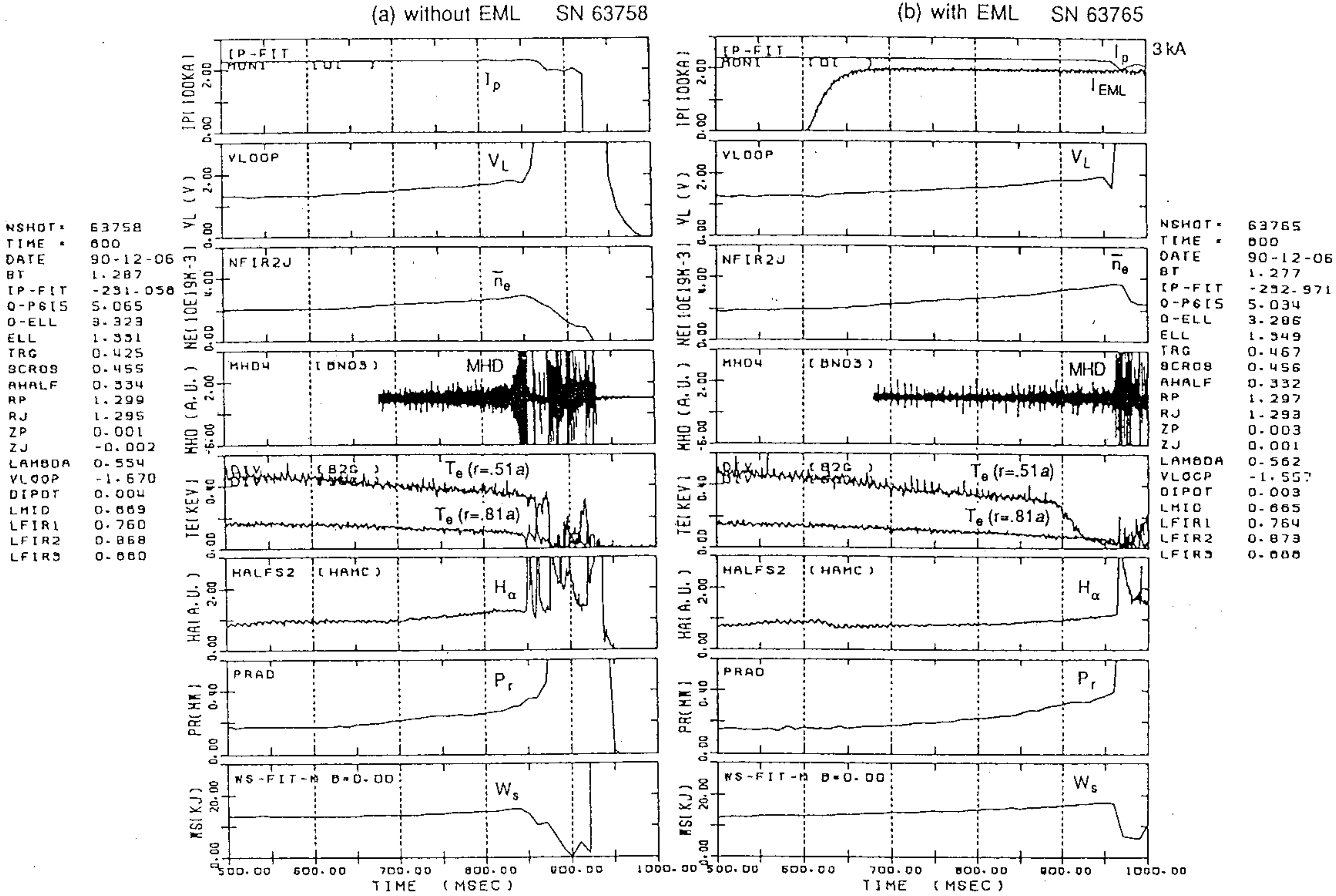


Fig. 3 Temporal evolution of plasma parameters (a) without EML and (b) with EML of low-m/even mode. Parameters are plasma current and EML coil current, loop voltage, averaged electron density, MHD activity, electron temperature at r=0.51$a$ and r=0.81$a$, $H_\alpha$ emission, radiation loss, and stored energy, from the top box by turns.

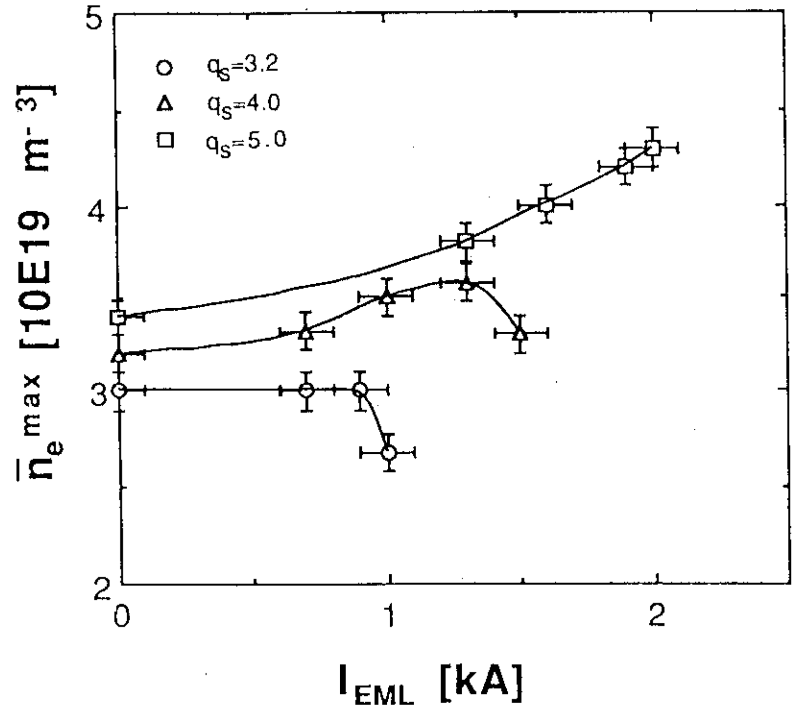


Fig. 4 Dependence of the maximum attainable density on EML current. Plasma current is 230kA, and EML operates with low-m/even mode (m/n=7/2). The plasma surface q is scanned at 3.2 (circles), 4.0 (triangles), and 5.0 (squares).

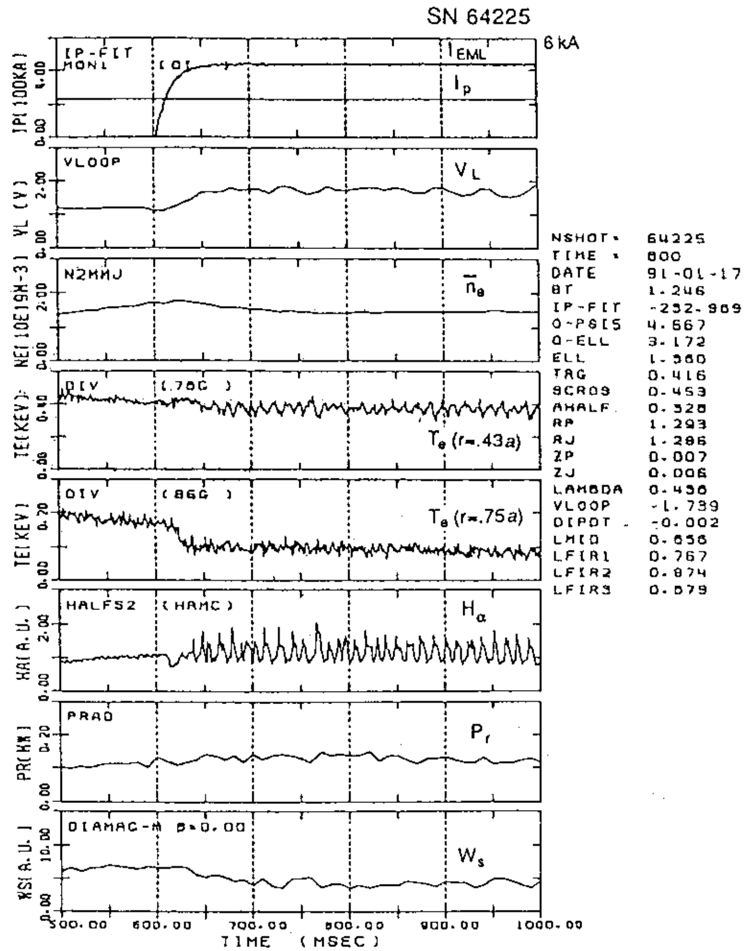


Fig. 5 Temporal behaviour of plasma parameters with EML of low-m/even mode. Surface q is 4.7. Parameters are plasma current and EML coil current, loop voltage, averaged electron density, electron temperature at r=0.43$a$, and that at r=0.75$a$, $H_\alpha$ emission, radiation loss, and stored energy, from the top box by turns.

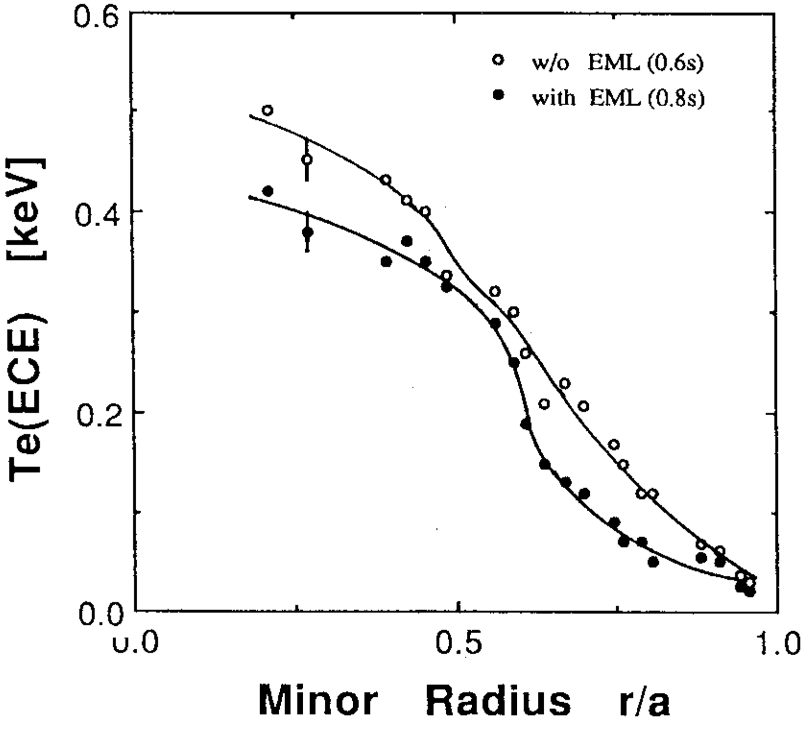


Fig. 6 The profile of electron temperature measured by electron cyclotron emission for the shot shown in Fig. 5. Open and solid circles show the temperature averaged over 10ms without EML (t=0.6s), and that with EML (t=0.8s), respectively.

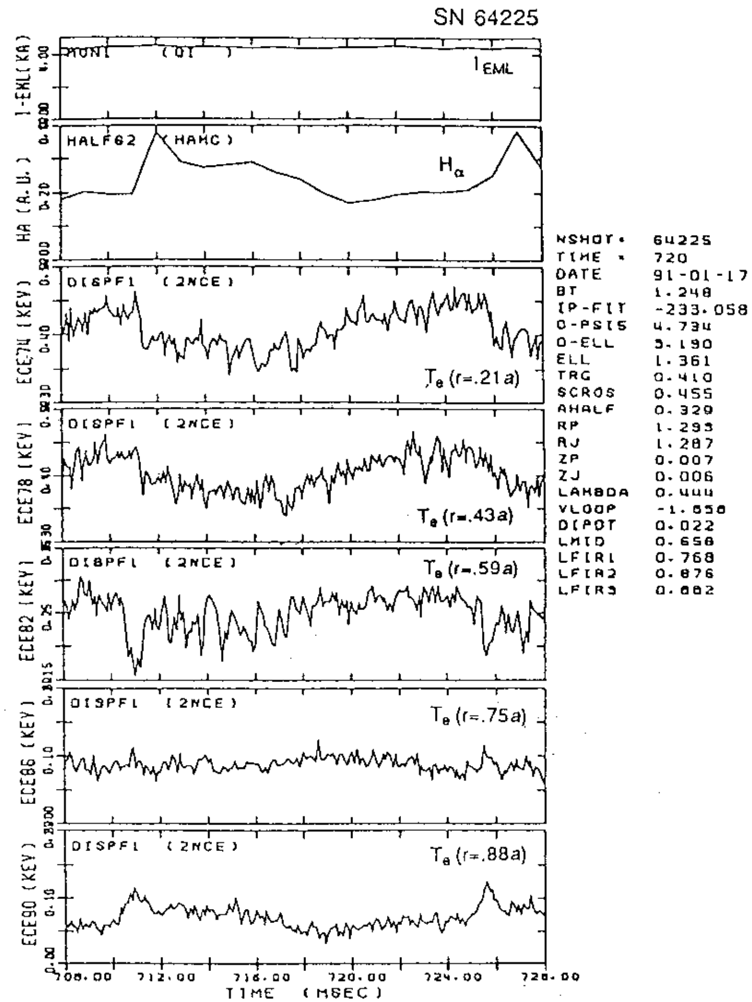


Fig. 7 Temporal behaviour of EML coil current, $H_\alpha$ emission, electron temperature at r=0.21*a*, r=0.43*a*, r=0.59*a*, r=0.75*a*, and r=0.88*a*, from the top box by turns. Time scale is from 0.708s to 0.728s.

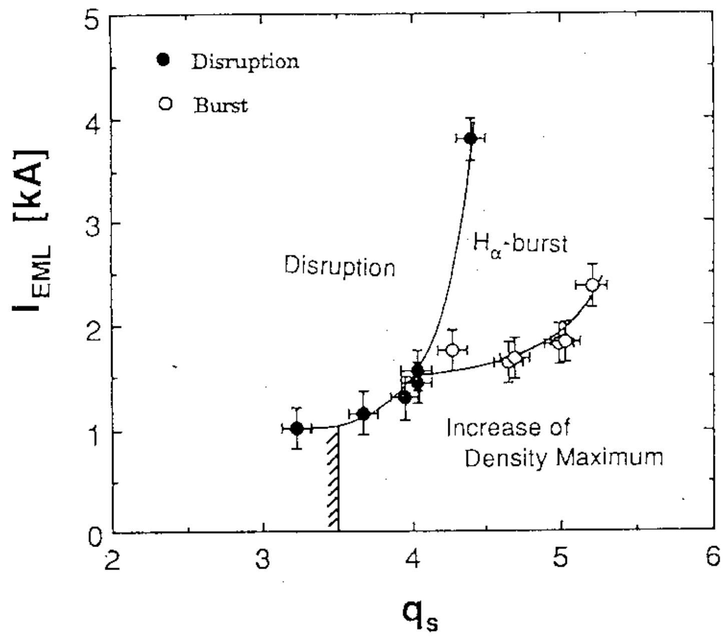


Fig. 8 Regions of the increase of maximum density, appearance of $H_\alpha$-burst, and major plasma disruption in the plane of EML current ($I_{EML}$) versus the plasma surface q($q_s$). Plasma current is 230kA, and EML operates with low-m/even mode. Open and solid circles show the marginal EML coil current for the appearance of $H_\alpha$-burst and for the plasma disruption, respectively. Hatched area indicates no improvement of density limit.

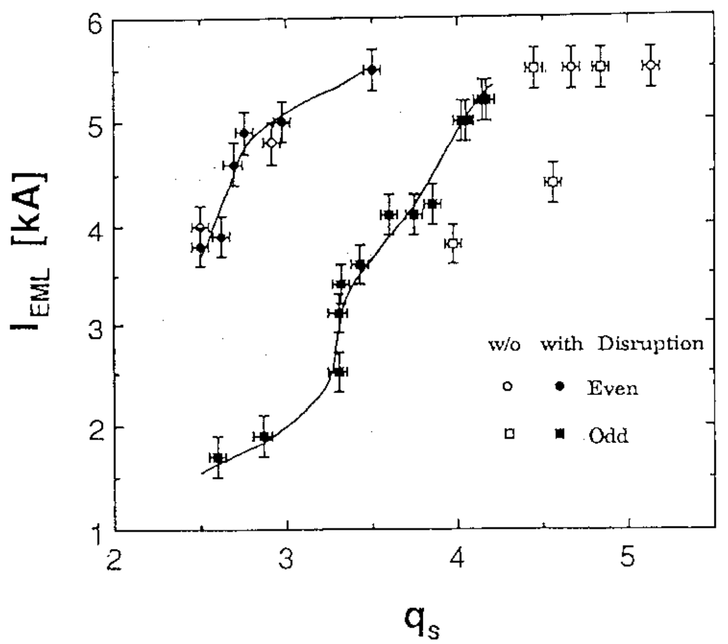


Fig. 9 EML current with high-m mode versus the plasma surface q. Plasma current is 230kA. Circles and squares represent the toroidal mode of even, and odd number, respectively; open and solid symbols indicate the case without, and with disruption, respectively.

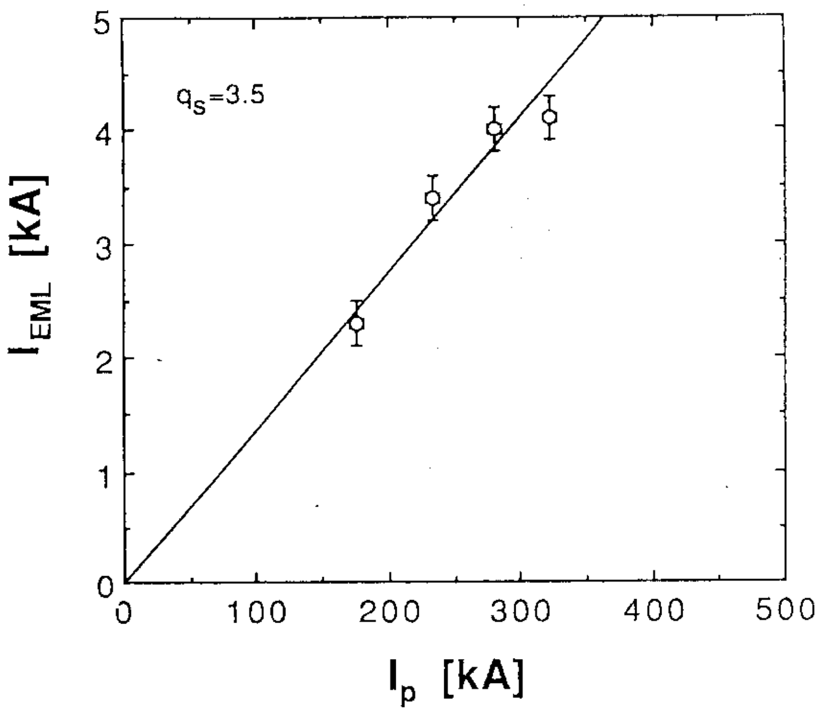


Fig. 10 Minimum EML coil current for the disruption versus the plasma current in the case of the EML with high-m/odd mode. Plasma surface q is fixed at 3.5.

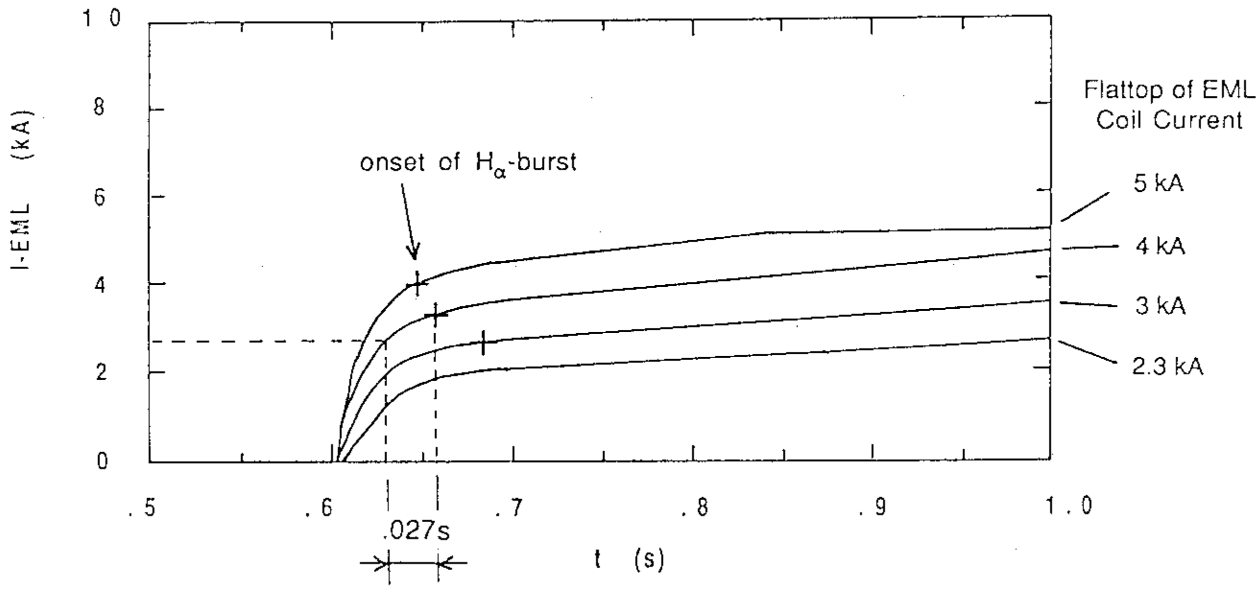


Fig. 11 Temporal evolution of EML coil current for the cases of the flat top current or 5kA, 4kA, 3kA, and 2.3kA, with low-m/even mode. Crosses show the time point of the onset in $H_\alpha$-burst. Flat top coil current is shown at the right side.